Volume 1
Number 4
October 2022
Pages 393–596

Environmental Science Advances

rsc.li/esadvances

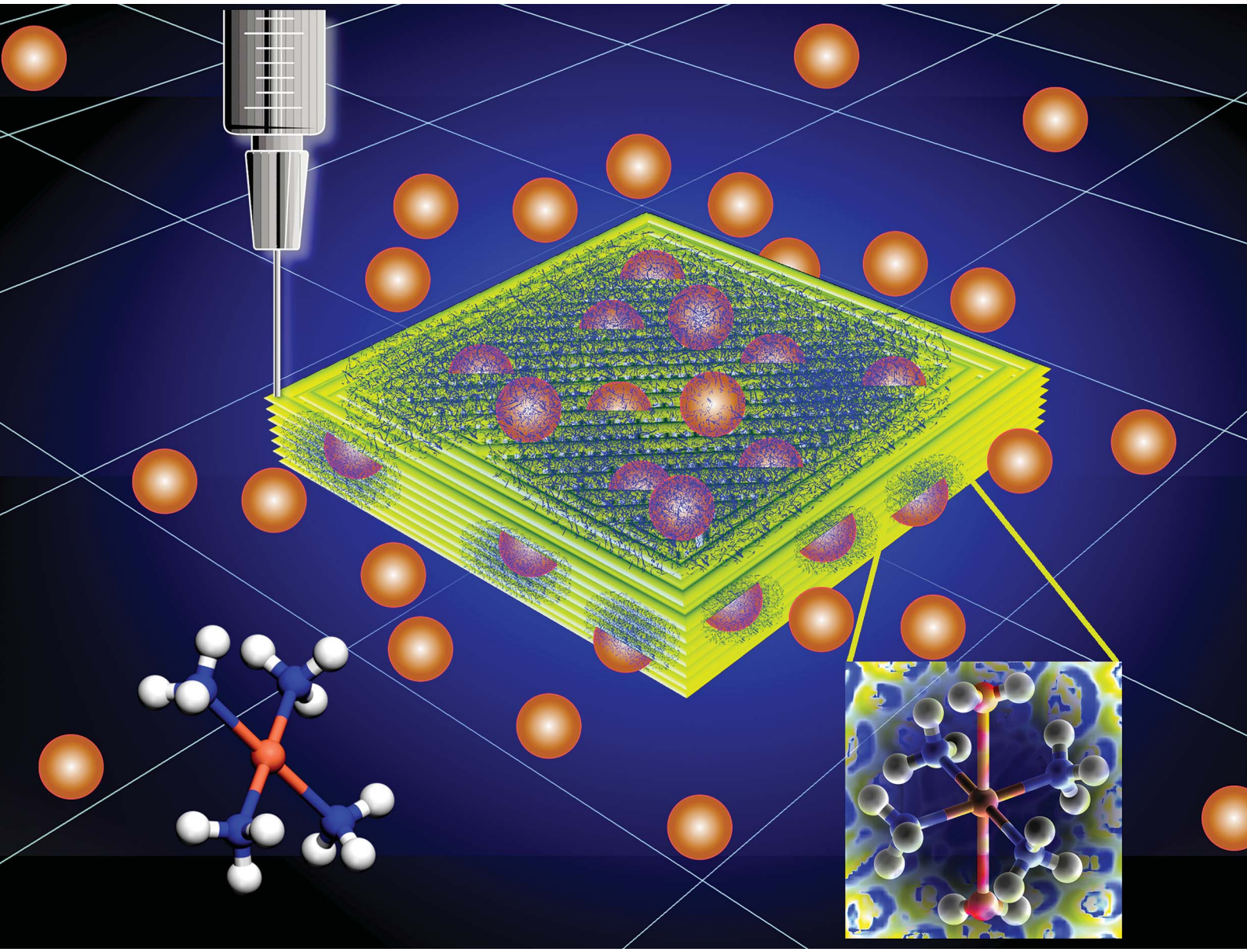

ISSN 2754-7000

ROYAL SOCIETY OF CHEMISTRY

PAPER
Silvana Andreescu *et al.*
3D printable polyethyleneimine based hydrogel adsorbents for heavy metal ions removal

Environmental Science Advances

ROYAL SOCIETY OF CHEMISTRY

PAPER

View Article Online
View Journal | View Issue

Cite this: *Environ. Sci.: Adv.*, 2022, **1**, 443

3D printable polyethyleneimine based hydrogel adsorbents for heavy metal ions removal†

Abraham Samuel Finny, Nadia Cheng, Oluwatosin Popoola and Silvana Andreescu *

Heavy metal contamination is one of the leading causes of water pollution, with known adverse effects on human health and the environment. This work demonstrates a novel custom-made 3D printable eco-friendly hydrogel and fabrication process that produces stable biocompatible adsorbents with the ability to capture and remove heavy metals from aqueous environments quickly and economically. The 3D printable ink contains alginate, gelatin, and polyethyleneimine (PEI), which binds heavy metals through primary and secondary amine side chains favoring heavy metal adsorption. The ink's rheological properties are optimized to create mechanically stable constructs, in the form of 3D-printed tablets, fabricated entirely by printing. The optimized tablets have high porosity and accessible surface area with multiple binding sites for heavy metal ion adsorption while the printing process enables rapid and affordable production with the potential for scale-up. The results demonstrate the contribution of hydrogel composition and rheology in determining the printability, stability, and heavy metal binding characteristics of the hydrogel, and indicate the critical role of the PEI in increasing stability of the printed construct, in addition to its metal binding properties. The highest removal capacity was obtained for copper, followed by cadmium, cobalt, and nickel ions. In the optimized formulation, each hydrogel tablet removed 60% from 100 ppm copper in 5 h and up to 98% in 18 h. For more concentrated solutions (1000 ppm), ~25% of copper was removed in 18 h. The printed tablets are stable, robust, and can be produced in a single simple step from inexpensive biomaterials. The ink's tunability, excellent printability, and stability offer a universally applicable procedure for creating hydrogel-based structures for environmental remediation. These unique capabilities open new avenues for manufacturing tailor-made constructs with integrated functionality for water treatment and environmental applications.

Received 21st May 2022
Accepted 30th May 2022

DOI: 10.1039/d2va00064d

rsc.li/esadvances

Environmental significance

Hydrogel-based adsorbents offer excellent opportunities for the development of eco-friendly technologies for heavy metal ions removal. In this study, an additive manufacturing technique is reported that provides an easy and effective way to rapidly and reproducibly fabricate structured 3D printing hydrogel-based adsorbents for environmental remediation. The results indicate the importance of achieving multifunctionality through reinforcing the hydrogel with PEI and establishes the essential role of hydrogel composition and rheology in determining the printability, stability, functionality and metal binding capacity. An improved understanding of the factors regulating the stability of these hydrogels will allow further development of 3D printable formulations and additive manufacturing techniques for a variety of water treatment and environmental applications. The 3D printing technique described here offers a cost effective, scalable and facile approach to create tunable adsorbents for use in environmental remediation that can be used broadly by the environmental community to custom-made 3D printed structures for environmental removal and sensing applications. This work can contribute to the development of bio-based methods for environmental remediation to achieve the global WHO goals for clean and sustainable water.

1. Introduction

Globally, heavy metal pollution with metals such as copper, nickel, mercury, cadmium, lead, and chromium is a significant environmental and health hazard, recognized by the World Health Organization (WHO) as a critical problem with significant consequences worldwide.[1,2] Heavy metals cannot be biodegraded; they are toxic and carcinogenic, and the potential for human exposure is high.[3] Electroplating, mining, tanneries, painting, and semiconductors are a few of the industries that are significant sources of heavy metal pollution. Others include livestock manure, fertilizers, herbicides, atmospheric deposition, and irrigation with polluted wastewater.[4] As a result of heavy metal pollution, plants experience oxidative stress, cellular damage, and disruption of respiratory and

Department of Chemistry and Biomolecular Science, Clarkson University, Potsdam, New York 13699-5810, USA. E-mail: eandrees@clarkson.edu; Fax: +49 315 268 6610; Tel: +49 315 268 2394

† Electronic supplementary information (ESI) available. See https://doi.org/10.1039/d2va00064d

photosynthetic activity,[5] the intake of crops contaminated by root transfer from soil to plant tissues can pose substantial health risks for humans.[4,6] Excess metal concentrations in soil alter food quality, leading to various disorders.[7] High levels of heavy metals such as copper, cadmium, nickel, and cobalt have been attributed to increased occurrences of cancer and industries that release an excess of these metal ions are known to pollute the environment.[8]

Since heavy metals are not usually degraded by natural processes, they can persist in the environment for a long time. Soil, water, and air are directly impacted by heavy metal contamination. Water runoff from factories, agricultural farms, and water treatment facilities in cities, villages, and towns can transport heavy metals, which eventually accumulate in water bodies, and river beds and is extremely hazardous to the local ecosystem.[9] Particulate matters of heavy metals that are discharged from anthropogenic sources and natural sources cause corrosion, haze, eutrophication, and even acid rains that can further pollute water bodies and soil.[10] Improper waste disposal and landfills, mining, and drilling can pollute soil by resulting in high heavy metal levels, that are further absorbed by living organisms and affect water quality.[11] Copper ions (Cu^{2+}) for example are used heavily in agriculture as an antifungal agent and can enter the water from the electroplating and mining industries.[12] The discharge of these wastes in streams, lakes, and groundwater reservoirs is responsible for health problems in humans and plants. The average Cu^{2+} concentration in soil ranges from 5 to 70 ppm but can reach 100 to 1500 ppm in the soil around vineyards where Cu^{2+} treatments are used to reduce the growth of mildew.[13] In sediments found in bays and estuaries, the Cu^{2+} concentration is less than 50 ppm, but polluted sediments may contain several thousand ppm. Around 4500 ppm of Cu^{2+} was reported in the soil around a Cu/Ni smelter.[14] The presence of high concentrations of heavy metals in polluted environments requires efficient and economical ways to remove them to ensure pollutant-free water.

Multiple techniques can be used to remove heavy metals from the water.[15,16] These include chemical precipitation, electrochemical reduction, membrane separation, and adsorption.[16] Though chemical precipitation is low-cost and straightforward,[15] the method generates significant waste, leading to secondary pollution. Electrochemical methods are rapid and provide good reduction yields, but the initial capital investment is high, and the technique requires an expensive electrical supply restricting broad applicability.[15] Due to low cost and easy operation, adsorption on different materials ranging from activated carbon to mesoporous and nano-based sorbents is the most broadly for removing contaminants from the wastewater.[17] Despite many adsorbents for the removal of heavy metals, only a fraction of those is eco-friendly. Recently, hydrogel-based adsorbents have gained interest as they are inexpensive, made from abundant materials and are effective for heavy metals removal. Compared to other adsorbents, hydrogels can absorb heavy metals within their three-dimensional, highly porous network, thereby providing more sites per unit volume for adsorption, leading to high adsorption efficiency.[18,19] Herein, we introduce 3D printing as an additive manufacturing technique for fabricating stable custom-made biopolymer-based adsorbents incorporating alginate, gelatin, and PEI to form structured hydrogels, in the form of 3D-printed tablets, to remove heavy metals ions, *e.g.*, copper, cadmium, cobalt, and nickel, from aqueous environments.

3D-printing technology has attracted much interest because of its ability to customize and tailor macrostructures of different materials for a variety of applications.[20] 3D printing allows digital computer-aided designs to be quickly turned into 3D objects by successfully printing customized inks directly guided by computer models.[21,22] 3D printed hydrogels have been widely investigated in the biomedical field for organ printing and tissue engineering. Despite their potential to create environmentally friendly bio-based sorbents in a customizable way, 3D printing has been scarcely used for environmental remediation applications.[23] Bioprinting through extrusion provides a more straightforward, flexible, and inexpensive manufacturing process, where the "ink" is extruded layer by layer through fine nozzles until a stable and orderly structure is achieved. Therefore, the assembly of biopolymers into hydrogel adsorbents with ordered macrostructures using 3D printing technology is a promising approach for preparing hydrogel adsorbents. Hydrogels made of natural biopolymers such as alginate, chitosan, and gelatin are among the most amenable classes of 3D printable bioink materials.[24] These biopolymers are easily accessible, biocompatible, and due to their functionalities, have a high sorption capacity for heavy metals binding, making them excellent candidates for environmental remediation.

Herein, we report a tertiary hydrogel adsorbent system uniquely suited for 3D printing, with excellent shear-thinning properties and thermodynamic stability and the capability to remove metal ions from environmental water samples (Fig. 1). The hydrogel is made of alginate and gelatin, which provide an ideal 3D printable ink composition amenable to printing. Sodium alginate, a hydrophilic polysaccharide, is used due to its gel-forming characteristics, while gelatin provides strong crosslinking properties and good thermal stability.[25,26] While alginate is known for its ability to uptake metal ions through chelation, electrostatic, and ion exchange interactions,[27] its binding ability is limited and alginate hydrogels lack stability in aqueous environments. Here we show that polyethyleneimine (PEI) forms a homogenous PEI-based cross-linkable network with alginate with high chelation ability and stability in aqueous environments. The as-prepared metal-chelating ink can be directly 3D printed into stable constructs in a single-step process. The PEI's branched cationic polymer with rich primary, secondary, and tertiary amino groups has the ability to form complexes with metal ions such as Co^{2+}, Cu^{2+} and Cr^{3+},[28] making this composition an ideal candidate for heavy metal capture and removal. It is worth noting that PEI is water soluble and by itself cannot be used as a heavy metal adsorbent, limiting its applicability for environmental remediation. The 3D printed PEI-based structures reported here are physically stable, have high porosity, and high accessible surface area providing multiple binding sites for heavy metal removal. This adsorbent offers a practical and cost-effective method to remove metals from aqueous solutions with excellent sorption performance.

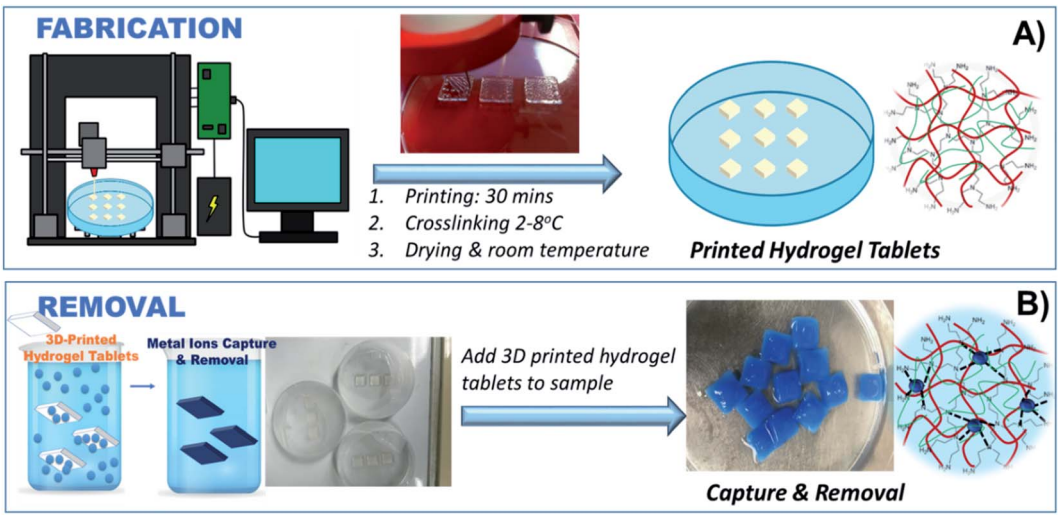

Fig. 1 Representation of the one-step 3D-printing fabrication (A) and removal (B) process of the hydrogel tablets, showing the interaction between PEI and Cu^{2+} ions, as an example. The hydrogel turns blue in the presence of Cu^{2+} due to the chelation process leading to the formation of cuprammonium complexes within the printed hydrogel.

The optimized printing composition and manufacturing process can be used to establish design principles for fabricating hydrogel-based adsorbents prepared by advanced manufacturing techniques. This work can contribute to the development of bio-based methods for environmental remediation to achieve the global WHO goals for clean and sustainable water.

2. Experimental section

2.1 Materials and methods

All chemicals were obtained from commercial sources and used as received. Sodium alginate NF MW 222.00 (Spectrum Chemical), gelatin from porcine skin gel strength 300 Type-A (Sigma Aldrich), and branched polyethyleneimine (PEI) from Aldrich were used to prepare the 3D printable adsorbent ink. Deionized (DI) water with a resistivity of 18.2 MΩ was obtained with a MiliQ system (Millipore). Copper(II) nitrate trihydrate (Acros Organics), nickel(II) nitrate hexahydrate (Aldrich), cobalt nitrate (J.T Baker), lead(II) nitrate (Mallinckrodt), and cadmium nitrate (Spectrum chemical) were used to prepare the corresponding metal ion solutions. An environmental water sample was collected from the banks of the Raquette River, Potsdam, NY.

Rheology tests were performed with a Modular Compact MCR 302 rheometer (Anton Paar). An adequate amount of sample was transferred onto the measuring platform of the rheometer, and the testing was performed using a measuring cone (CP50-1, D: 50 mm; angle: 1°). Nanoindentation experiments were conducted using a nanomechanical-testing instrument (TI950 Triboindenter, Hysitron Inc.) in displacement control mode with a Berkovich tip attachment at room temperature (RT). Tensile testing was conducted using a Mark-10 model no. BG20 Force Gauge with a maximum capacity of 100 N and a MARK-10 ESM 301 motorized test stand with a max load capacity of 1.5 kN. The heavy metal ion concentrations before and after adsorption were measured using PerkinElmer AAnalyst 600 Atomic Absorption Spectrometer.

The Brunauer–Emmett–Teller (BET) gas sorption measurements were performed at 77 K under nitrogen using a Quantachrome Autosorb IQ analyzer, with prior overnight degassing of the samples at 100 °C. Before analysis, the freshly prepared hydrogel tablets were soaked in ethanol for 6 h (the ethanol was replaced at every 2 h), followed by the supercritical CO_2 activation using a Tousimis Samdri PVT-3D critical point dryer.

To visualize the structure and porosity of the tablets before and after exposure to metal ion Scanning Electron Microscopy (SEM) was used to study the morphology of hydrogels. For SEM analysis, the hydrogel tablets were immersed in liquid nitrogen and, once completely frozen, they were lyophilized for 48 hours. These samples were then attached to an SEM holder and analyzed for morphology and porous structures on a JEOL JSM 7900-LV SEM.

2.2 Formulation of 3D printable adsorbent ink

The 3D printable adsorbent ink was formulated using an 8% sodium alginate solution prepared and mixed overnight using a Stir-Pak High-speed (Cole Parmer), low-torque overhead mixer motor (23–2300 rpm), along with a Fisher Scientific Isotemp Stirring Hotplate with a temperature controller thermocouple. Sodium alginate of 8% was used in this study as it was found that levels lower than 8% lead to very low viscosity solutions that were not suitable for printing. At 21 °C, 2% alginate had a viscosity of 6400 mPa s, while 4% had 44 800 mPa s and 8% had 5.40×10^5 mPa s. A 10% gelatin solution having a viscosity of 1.21×10^6 mPa s was prepared using a vortex mixer. This gelatin solution was transferred to a beaker containing 8% sodium alginate solution and further mixed for 1 hour to form a mixture of alginate–gelatin in a 9 : 1 ratio. The alginate–gelatin combination formed the base ink for 3D printing. The optimized heavy metal removal ink was created by adding 5 ml

of PEI solution (50 mg ml^{-1}) to the 45 ml of base alginate–gelatin ink. The three-polymer component mixture was mixed for 2 hours to get a homogenous 3D printable adsorbent ink. For printing, the ink was transferred into a syringe-cartridge fitting the Allevi 2 bioprinter and centrifuged at 2000 RPM for 7 minutes to remove air bubbles. For making an optimal ink formulation, various concentrations of alginate, gelatin, and PEI were tested alone and in different ratios. Their viscosities were characterized with respect to temperature. The rheological properties and the temperature-dependent viscosity changes determine the printability of the ink and stability of the 3D printed constructs, as discussed in the results section.

2.3 3D printing models and printing process

3D models were created using Autodesk software, primarily AutoCAD and Inventor. The computer-generated 3D models were processed by 'slicing' using Repetier-Host and uploaded to the Allevi 2 3D Bioprinter. The ink was transferred to 10 ml cartridges (BD Luer-Lok tip), and different dispensing tips (Small Premium Dispensing Tip Kit – JG120DN-NT, Large Dispensing Tip Kit – JG120NK from Jensens) were attached to the cartridge and then tested for printability. The cartridge was centrifuged at 2000 rpm with an endcap to remove any air bubbles before printing. Printing parameters were optimized to create optimal configurations that were finally used to fabricate the 3D printed hydrogel tablets (Fig. 2). The printing procedure was further optimized by adjusting the printing pressure, tip diameter, and the 3D printer application settings until stable printed constructs were obtained. The weight of the tablets was 0.68 ± 0.072 g in dry state.

2.4 Heavy metal ions removal

Optimization experiments of the 3D printed hydrogel tablets to determine removal efficiency were first carried out with Cu^{2+}. For testing the Cu^{2+} removal performance, the printed hydrogel tablets were immersed in Petri dishes containing 40 ml Cu^{2+} solutions of variable concentrations (100, 250, 500, 750 and 1000 ppm). For each Cu^{2+} concentration, the tests were performed at least five times. Sample solutions were analyzed for residual Cu^{2+} content at the following time intervals: 1, 2, 5, and 18 hours. The 3D printed tablets were then tested with four other heavy metals, cadmium (Cd^{2+}), cobalt (Co^{2+}), nickel (Ni^{2+}), and lead (Pb^{2+}), individually using an identical procedure with one tablet per vial as that used for Cu^{2+} and exposed to each metal ion for 18 h. Petri dishes were filled with 40 ml of 100 ppm of Cd^{2+}, Co^{2+}, Cu^{2+}, Ni^{2+}, and Pb^{2+} solution, respectively. For the determination of the selectivity of the method for heavy metals, a study was performed where a 40 ml mixture containing 100 ppm each of Cu^{2+}, Cd^{2+}, Co^{2+}, and Ni^{2+} was exposed to hydrogel tablet, and the residual concentration of each of these ions was determined using atomic absorption spectroscopy after 18 hours of exposure.

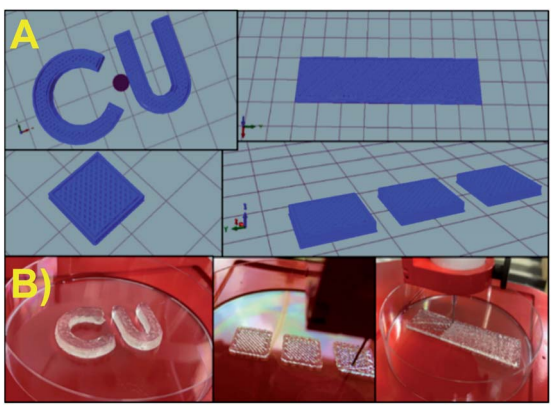

Fig. 2 3D models created using Autodesk (A) and printability of the alginate–gelatin–PEI ink showing printing of different shapes: Cu, square, and rectangle (B). Shown here as an example for Cu^{2+}; other structures can be created using similar processing.

2.5 Application to an environmental water sample

The practical utility of the tablets was tested in environmental water samples, and their efficiency was established for Cu^{2+} removal. The water was collected from Garner Park, Potsdam, NY, and used as-is. Petri dishes with a single hydrogel tablet were used during this study. The sample (40 ml) was spiked with Cu^{2+} to create a 100 ppm solution. After 18 hours of exposure, the samples were analyzed by AAS to determine the residual Cu^{2+} content.

3. Results and discussion

3.1 Formulation of 3D printable hydrogel adsorbent ink and printability

The formulation of ink is crucial for developing compositions that are 3D printable and suitable for creating robust and mechanically stable constructs maintaining their functionality for heavy metal removal in aqueous environments. Hydrogels consisting of 3D crosslinked polymer networks are known for their printability but obtaining robust and reproducible printed constructs requires optimized composition, viscosity, miscibility, structure, and a rheological behavior of the formulation that is amenable to printing.[22,29] Multicomponent polymer mixtures have been traditionally used for 3D printing and are known to provide good gelation properties and viscosity, as opposed to single polymeric systems. However, obtaining miscible single-phase mixtures that are thermodynamically stable can be challenging, and their printing and gelation behavior is difficult to predict. The selection of printing materials is thus critical for ensuring compatibility and preventing phase separation and cracking, which are necessary to achieve printability.

To formulate the adsorbent ink, we had the following considerations: (1) the ink should exhibit a good pseudoplastic (shear thinning) behavior to enable extrusion through the printer nozzle such that it enables a layer-by-layer printing; (2) the base materials of the ink should have tunable viscosity; (3) the composition of the ink, crosslinking conditions and printing time should enable solidification/gelation within a reasonable time to enable well-defined stable constructs; (4) one of the ink components should have specific binding or

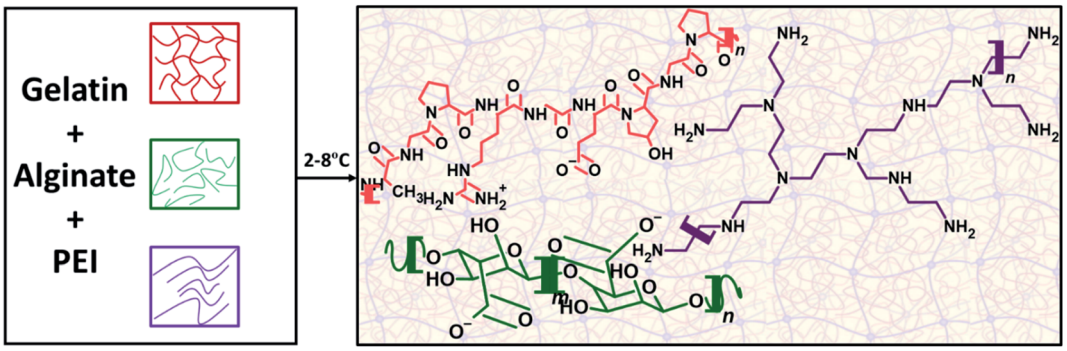

Fig. 3 Mechanism of physical crosslinking of alginate, gelatin, and polyethyleneimine in the formulation of the hydrogel adsorbent.

chelation ability for metal binding, and: (5) the printed construct should be mechanically stable in aqueous environments to prevent leaching of captured ions. Because of their biocompatibility and good mechanical properties, alginate and gelatin have been standard choices for the fabrication of hydrogels, particularly for applications in biomedicine and 3D bioprinting.[21,22,25,30–32] In this work, we utilized the interaction between the macromolecular chains of gelatin and anionic polysaccharide sodium alginate, which leads to the formation of polyelectrolyte complexes through hydrogen bonding and electrostatic interactions between the negative carboxylate groups of alginate and the positive nitrogen groups in gelatin.[33] The hydrogen bonding between the OH groups in alginate and the NH groups in gelatin provides a stable hydrogel network forming a base for the primary ink (Fig. 3). To further impart functionality for heavy metal removal, the PEI, a known polymer with abundant primary and secondary amine side chains favoring heavy metal ion adsorption[28,34] has been added to the base ink. In addition to providing metal removal, the branched PEI has the ability to interact with alginate even at low degrees of ionization and homogenously reinforce alginate hydrogels, further improving their stability and preventing alteration of the pore structure.[35] Despite the commonality of these polymers, there have not been any studies on the printability of these polymer composites, the stabilization of the PEI within alginate hydrogels and their characteristics for heavy metal removal. To understand the printability and gelation properties, we studied the gelation behavior of each component individually and then in mixtures with respect to temperature.

Fig. 4 shows the viscosities of various hydrogel compositions with respect to temperature (°C) when shear rates of 1 s^{-1} and 2 s^{-1} respectively are applied. At 20 °C and a shear rate of 1 s^{-1}, the viscosity values were: 717.80 Pa s for alginate, 327.88 Pa s for gelatin, 854.36 Pa s for the alginate–gelatin composite, and the highest value of 1148.70 Pa s for the three-component adsorbent ink. The viscosity of alginate alone does not vary significantly when the temperature is changed. By comparison, the viscosity of the gelatin begins to show a drastic downward trend at 35 °C for both shear rates. When gelatin and alginate are mixed, the viscosity decreases much slower with the increase in temperature in comparison with alginate and the gelatin alone. For example, at 50 °C, the viscosity of alginate is 394.74 Pa s, that of gelatin is 0.01 Pa s, and the viscosity of the alginate and gelatin composite is 307.69 Pa s, When PEI is added, the viscosity of the adsorbent ink decreases slower than the alginate–gelatin indicating a value of 365.00 Pa s, demonstrating enhanced stability and a reinforcement effect when PEI is used. The same trend was observed when a higher shear rate of 2 s^{-1} was applied, indicating stability in the composites' rheological response at a higher shear rate. Therefore, the best printable configuration was achieved when combing alginate, gelatin, and PEI. It is interesting to note that in the absence of PEI when

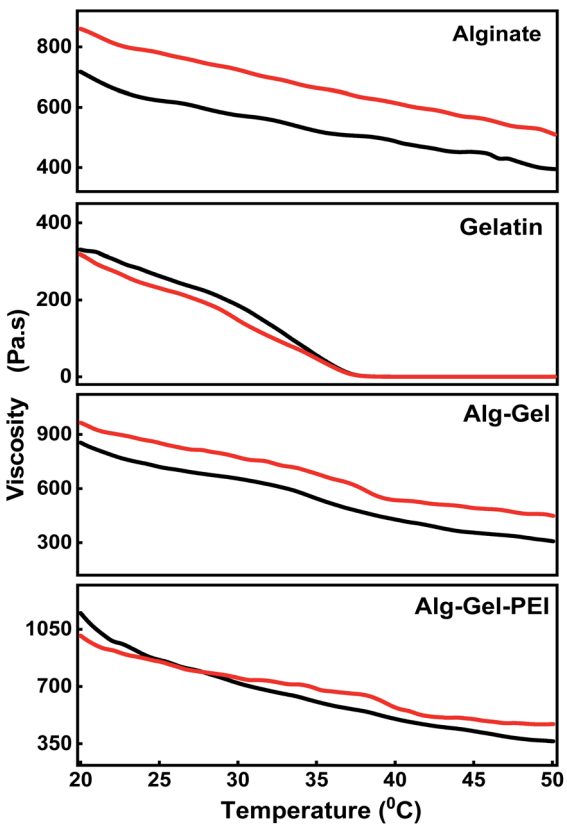

Fig. 4 The viscosity of alginate, gelatin, alginate–gelatin (Alg–Gel), and alginate–gelatin–PEI (Alg–Gel–PEI) hydrogel composites as a function of temperature (°C) at a shear rate of 1 s^{-1} (black) and 2 s^{-1} (red).

a binary alginate–gelatin composite was used, the printing of the mixture did not produce a stable construct; the printed hydrogel collapsed due to the lack of crosslinking, further supporting the critical role of the PEI to the gelation and printing process. The final composition displayed excellent printability and temperature stability between 20 °C to 50 °C. The BET surface area of the Alg–Gel–PEI was 9.907 $m^2\ g^{-1}$, comparable with other types of hydrogels: chitosan[36] or alginate/PEI based.[37]

The rheological tests shown in Tables S1 and S2 – ESI† support our hypothesis that the polymers used in this formulation are miscible, the three can co-exist in a single phase, and the mixture is thermodynamically stable.

3.2 Mechanical testing of 3D printed constructs

The mechanical stability of the 3D printed constructs created using the basic 3D model shown in Fig. 2 was tested by printing the hydrogel tablets, followed by drying and subjecting them to mechanical testing by nanoindentation. These tests were performed at twenty different points on the surface of the tablet, and the results were used to calculate the reduced elastic modulus and hardness at each of these points. Fig. 5 shows the corresponding load *versus* depth (displacement) curve and the different reduced elastic modulus and hardness at these points. Reduced elastic modulus represents the elastic deformation that the sample and the indenter tip undergoes as the indenter tip indents the sample. Reduced modulus was calculated using the following equation.

$$\frac{1}{E^*} = \frac{1-(v)^2}{E_1} + \frac{1-(v^1)^2}{E_2}$$

where: E^* = reduced modulus, E_1 = modulus of the specimen, E_2 = modulus of the indenter, v = Poisson's ratio of the specimen, and v^1 = Poisson's ratio of the indenter.

The load-depth indentation curves of the dried adsorbent tablets revealed the magnitude of indentation depth corresponding to the volume of the composite that was deformed due to the applied indentation force. From the graph, it can be clearly inferred that these hydrogel adsorbent composites can handle high amounts of applied forces and therefore can be used as high-performance materials. Based on the very low deviation between the reduced elastic modulus values for the twenty indentations and the hardness values across the points, it can be inferred that the formulation is homogenous and the distribution of the PEI across the hydrogel is uniform. Further bending, twisting, and tensile tests were conducted as shown in Fig. S1 and S2,† exhibiting excellent mechanical properties of the fabricated hydrogel tablets. The 3D printed band remained flexible and did not deform even after sequential bending at a 90° angle on each side 50 times (100 times in total) and twisting on each side 50 times (100 times in total) (Fig. S3†). The stability was maintained even when a uniaxial force of 100 N was applied along the length of the hydrogel tablet.

The next set of characterization experiments was performed to determine the porosity of the printed hydrogel and examine alterations in the pore structure as a result of metal ion complexation. These tests were run with the PEI-reinforced gelatin–alginate hydrogel before and after exposure to Cu^{2+} ions, selected here as an example. As shown in the SEM images obtained with frozen hydrogels (Fig. 6A, D and E), the surface of the hydrogel is highly porous, with micropores distributed evenly across the entire printed surface. The availability of

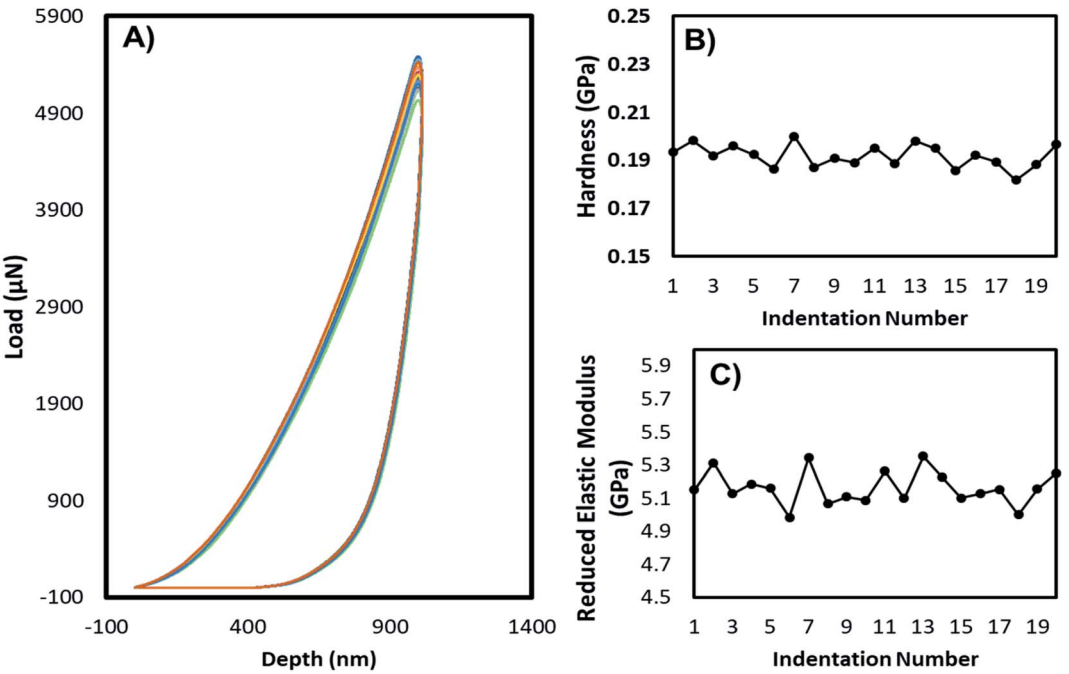

Fig. 5 Nanoindentation tests: (A) load *vs.* depth profile, (B) hardness, (C) reduced elastic modulus of the dried films prepared from alginate–gelatin–PEI composite.

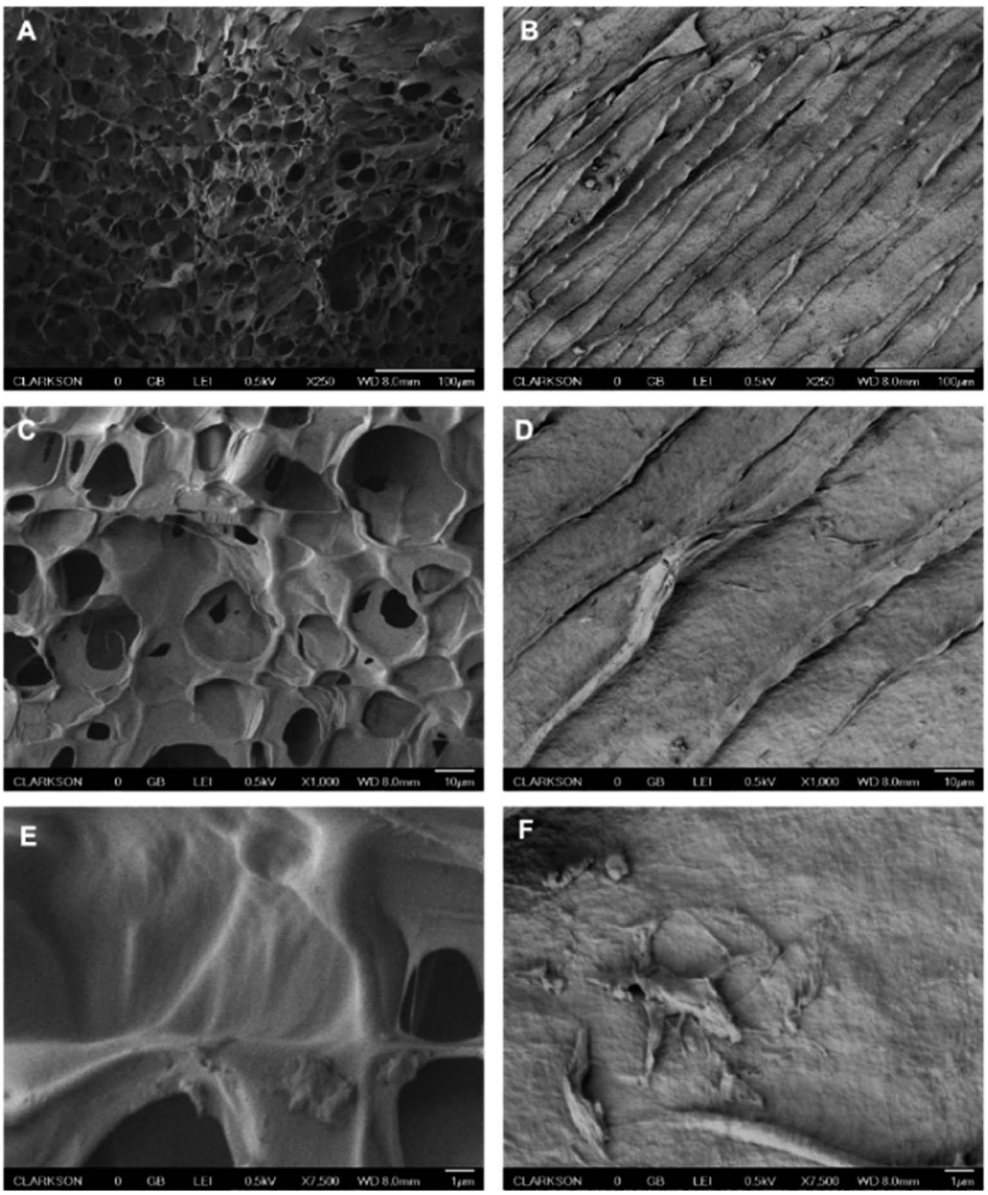

Fig. 6 SEM images of the 3D printed hydrogel tablets before (A, C, E) and after (B, D, F) exposure to 100 ppm Cu^{2+} at 250× (A, B), 1000× (C, D) and 7500× (E, F) magnifications.

a large number of pores provides a vast surface area for the interactions between Cu^{2+} and PEI. Incubating the gels with a Cu^{2+} solution led to a significant change in the hydrogel structure due to crosslinking between the Cu^{2+} ions and the PEI. Once crosslinking occurs, the pores close, and the hydrogel has a smooth, uniform surface, as shown in Fig. 6B, D and F.

The characterization tests demonstrate that our printing procedure produces highly porous and mechanically stable hydrogels, which could be used for environmental remediation applications. The significant microstructural alterations in the hydrogel pore structure seen by SEM after metal complexation further support our binding mechanism and demonstrate successful interaction between the metal ions and the hydrogel. Moreover, the tablets were highly stable and maintained their structure and morphology in environmental solutions and pH conditions ranging from 4 to 10. These materials and optimized printed constructs were further evaluated in batch adsorption tests to assess their performance for the removal of metal ions with laboratory standards and environmental water samples.

3.3 Metal ion removal studies

Tablet adsorption capacity, kinetics, and optimization of the incubation time were first determined by batch experiments with Cu^{2+}. Evidence of metal binding was first revealed by the visible micro-structural changes in the tablet, noticeable by the naked eye. After exposure to the Cu^{2+} solution, each tablet showed a narrowing of the edges and an immediate change in color from uncolored to blue (Fig. S4†). A slight shrinking in the tablet was also observed (Fig. 7). Continued exposure to the Cu^{2+} solution caused the entire table to change color to blue,

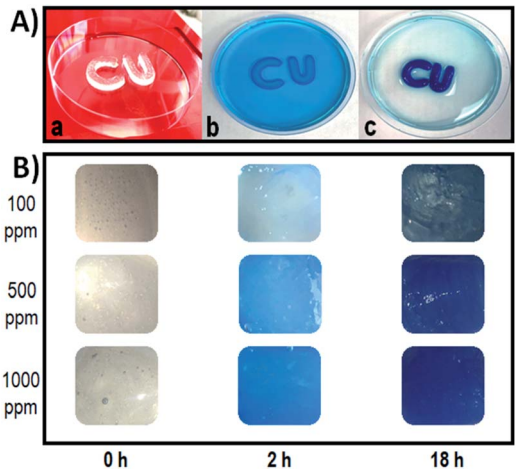

Fig. 7 (A) Illustration of the Cu^{2+} capture/removal with a 3D printed 'CU' construct showing the as printed tablet in the dry state (a), immersion into a Cu^{2+} solution of 500 ppb (b), and capture evidenced by a change in the color of the tablet to a dark blue over the time of exposure (c). Note the ability of the hydrogel tablet to capture Cu^{2+}, essentially concentrating it from the solution. (B) Color changes of square-printed hydrogel tablets before (0 hours) and after exposure to 100, 500, and 1000 ppm for 0, 2, and 18 h, respectively.

indicating a time-dependent adsorption process. Despite the morphological changes, the hydrogel remains functionally intact, mechanically stable, and does not dissolve in the aqueous environment during the exposure experiments. This behavior is attributed to the increased stability provided by reinforcing the hydrogel with the PEI and the complexation of PEI with the metal ions, increasing stability and robustness. These results are in line with the SEM results showing significant microstructural changes in the porous structure following exposure. The high stability in the aqueous environment, the low cost, and the biocompatibility of the hydrogel make these formulations attractive candidates for environmental applications.

Fig. 8 shows the results of batch adsorption experiments with the 3D printed tablets exposed to Cu^{2+} solution for 1, 2, 5, and 18 hours. To evaluate the removal capacity of the alginate–gelatin–PEI tablet over time, one or two tablets were incubated with high concentrations of Cu^{2+} of 100, 500, and 1000 ppm Cu^{2+}. During the experiments, the hydrogels started turning blue immediately after exposure to the Cu^{2+} solution indicating the formation of the cuprammonium complexes homogenously throughout the hydrogel tablet's body. Continued exposure caused the entire tablet to turn blue with higher Cu^{2+}

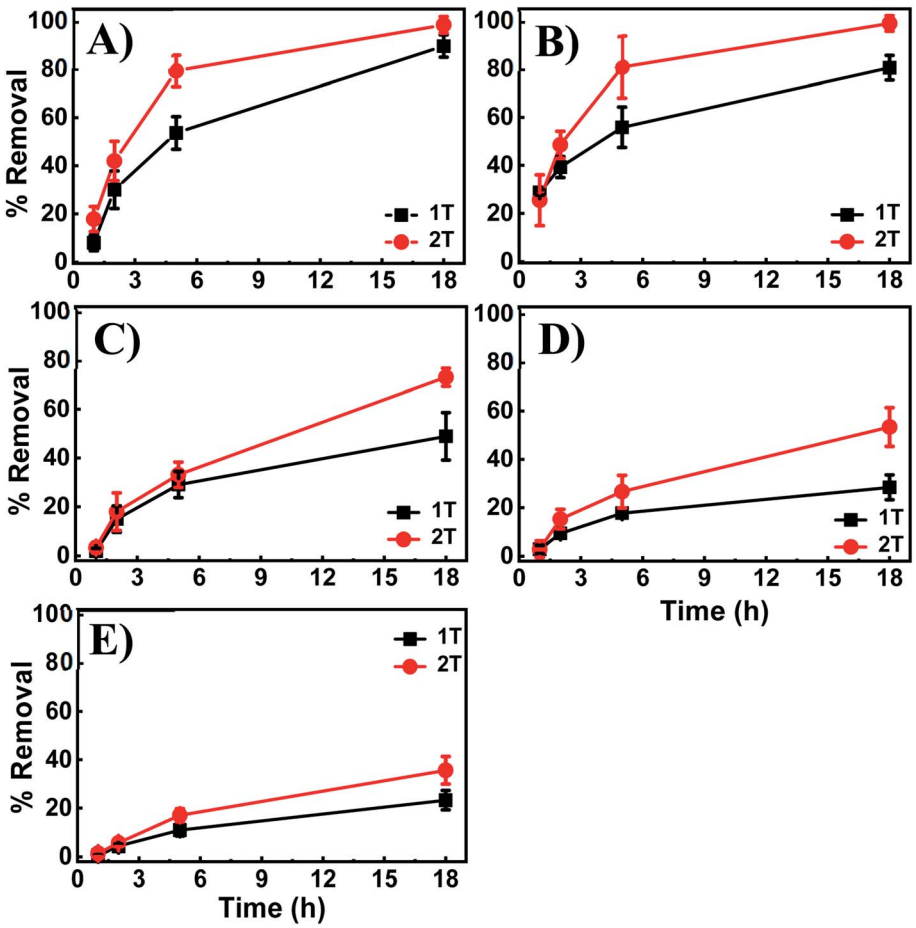

Fig. 8 Percent removal for Cu^{2+} *vs.* time with one (~0.68 g) hydrogel tablet (black) and two (~1.47 g) hydrogel tablets (red) after 18 hours incubation in Cu^{2+} solutions of the following concentrations: 100 (A), 250 (B), 500 (C), 750 (D), and 1000 (E) ppm.

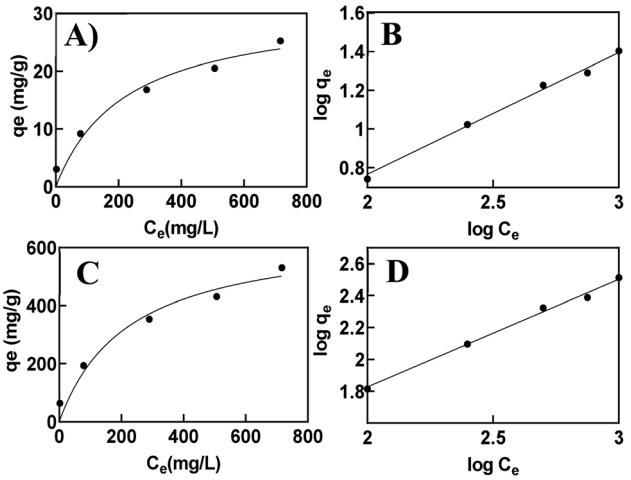

Fig. 9 Isotherm curves for the adsorbent in a hydrated *vs.* dehydrated state. Site specific binding (A, C) and Freundlich fit (B, D).

concentrations inducing a deeper color. Cu^{2+} removal begins immediately upon immersion of the tablet in the solution and proceeds gradually over time. Based on the AAS results of the residual Cu^{2+}, the amount of Cu^{2+} captured and removed per single tablet is significant. For example, when only one tablet was exposed to 100 ppm Cu^{2+} solution, 18.43% was removed after one hour, ~50% were removed for 5 hours, and the entire Cu^{2+} present was completely removed, *i.e.*, 100% removal, after 18 hours. When more tablets are used, the removal time decreases, and Cu^{2+} is more efficiently removed with a higher sorption capacity provided by the availability of more capture sites in the two tablets and a shorter time. The same trend was observed when higher Cu^{2+} concentrations were tested.

The kinetics of the adsorption process and calculation of the total adsorption capacity and binding isotherms were next evaluated using the Langmuir and Freundlich models. The site-specific binding fit was determined using the equation:

$$Y = q_e^{max} \frac{X}{K_d + X}$$

where: q_e^{max} is the maximum equilibrium binding/adsorption of Cu^{2+} per gram of the 3D printed adsorbent. This value is extrapolated to higher concentrations of Cu^{2+} to get the final value. K_d is the equilibrium dissociation constant, measured as the concentration (mg L^{-1}) of Cu^{2+} necessary to achieve a half-maximum binding/adsorption at equilibrium. The Freundlich fit was performed by plotting the log C_e (the equilibrium Cu^{2+} concentration in mg L^{-1}) *vs.* log q_e (mg of Cu^{2+} removed per g of adsorbent) using the equation:

Table 1 Site-specific binding and Freundlich isotherm parameters for Cu^{2+} removal

	Specific binding (best-fit values)		Specific binding (95% confidence interval)			Freundlich		
Adsorbent state	q_e^{max}, mg g^{-1}	K_d, mg g^{-1}	q_e^{max}, mg g^{-1}	K_d, mg g^{-1}	R^2	$1/n$	K_f	$R2$
Hydrated	43.52	800.4	28.9 to 109	329.4 to 3144	0.96	1.59	0.61	0.993
Dehydrated	633.20	1037.0	378.8 to 3562	370.1 to 9469	0.96	1.48	1.61	0.993

Table 2 Comparison of the removal capacity of the 3D printed alginate–gelatin–PEI with those reported with other hydrogel-type adsorbents for Cu^{2+} removal

Hydrogel composition	Manufacturing process steps and scalability	q_e^{max} (mg g^{-1}) Cu^{2+} adsorption	Ref.
Magnetic calcium alginate hydrogel beads	Gelation of alginate/Fe_2O_3 mixed suspension	159	38
Chitosan cellulose hydrogel beads	Droplet addition of chitosan into NaOH through a vibration nozzle system	53.2	39
MXene/alginate composite	A mixture of crosslinked MXene/ alginate by freeze-drying	87.6	40
Chitosan/PEI/graphene oxide	Cellulose membranes dip-coated in chitosan–PEI–graphene and glutaraldehyde in a multistep process	NA/90% removal of 20 ppm	41
Polyacrylamide/graphene oxide/ sodium alginate	Multistep free-radical polymerization, neutralization, and crosslinking	280.3	42
PEI/k-carrageenan composite (CG)	PEI/CG mixture dried under vacuum, freeze-dried into a mold	116	43
Alginate/gelatin–PEI	PEI-based hydrogen fabricated by one-step printing, fully automatic, and scalable	633.2/100% removal of 100 ppm	This study

$$\log q_e = \log k_f + \frac{1}{n} \log C_e$$

Because the printed hydrogel takes up a significant amount of water and swells in aqueous environments due to their hydrophilic groups in the backbone, the isotherms were calculated for both dry and hydrated state hydrogels (Fig. 9). The corresponding kinetic parameters are listed in Table 1. The plot of $\log C_e$ *vs.* $\log q_e$ shows a straight line, which suggests a Freundlich isotherm indicative of multilayer adsorption on a heterogeneous surface. Given the combined use of alginate–gelatin and PEI in our system, it is expected that metal ions binding to the printed hydrogel occur through multipoint interactions, including chelation to the PEI as well as electrostatic binding to the three-dimensional polymeric network. To further quantify binding and estimate a maximum saturation point for Cu^{2+} removal, we have also applied a site-specific binding fit, which allowed us to determine the maximum ion binding for dry and hydrated tablets (Table 1).

The maximum absorption capacity, q_e^{max} measured per gram of dehydrated sorbent of 633.2 mg g^{-1} is significantly higher than the adsorption capacity reported previously with other hydrogel-type sorbents based on similar biomaterials like alginate, chitosan, and cellulose. This extremely high sorption capacity supports our hypothesis of achieving increased binding efficiency due to the favorable adsorption with the porous functional structure of the 3D printed hydrogel network. A comparison of adsorption capacity, q_e^{max}, for the removal of Cu^{2+} ions using previously reported hydrogel-type sorbents is shown in Table 2, indicating superior adsorption of the 3D printed hydrogels. The high binding ability is attributed to the macroscopic pores and abundant surface functionality available for chelation, favorable for removing metal ions in aqueous environments.

3.4 Removal of other heavy metals

Further investigations were performed to evaluate the adsorption capacity of the 3D printed tablets and demonstrate broad applicability as a universal sorbent for metal ions removal. Experiments were carried out with the adsorbent exposed to 100 ppm of Cd^{2+}, Co^{2+}, Cu^{2+}, Ni^{2+}, and Pb^{2+} solutions. Fig. 10 provides cumulative results showing percent removal of each metal ion individually and in mixtures after 18 h incubation. The data indicate the ability of the tablets to remove in addition to Cu^{2+}, ions like Ni^{2+}, Cd^{2+}, Co^{2+} and Pb^{2+} with removal capacities of 90.38%, 59.87%, 46.27%, 38.66%, and 6.45% for Cu^{2+}, Ni^{2+}, Cd^{2+}, Co^{2+} and Pb^{2+} respectively. Comparative tests indicate the highest removal for Cu^{2+} and the lowest for Pb^{2+}. Of the metals investigated, Cu^{2+} and Co^{2+} cause the hydrogel to change color. In the presence of others, such as Ni^{2+}, the hydrogel remain pale white, despite displaying relatively high adsorption capacity (~60%).

To investigate if the hydrogel can remove multiple metal ions simultaneously or if they compete for the same binding sites,

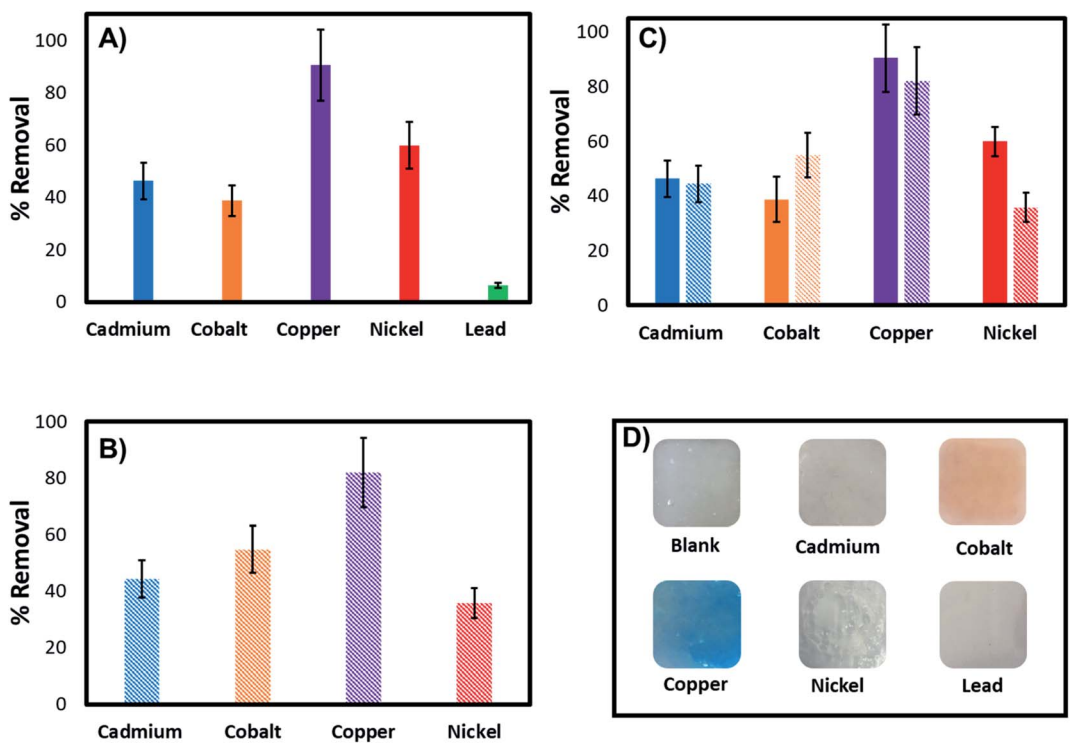

Fig. 10 Percent removal of heavy metals after 18 hours using five (A) and one (B) tablets exposed to 100 ppm concentration of a particular heavy metal, individually. Each tablet weighed approximately 0.7 g. (C) Comparative analysis of heavy metal removal capability of one hydrogel tablet placed in an aqueous solution containing each individual heavy metal (solid bars) *vs.* a mixture of the four metals (striped bars). (D) Image of hydrogel tablets exposed individually to 100 ppm metal solutions after 18 hours using one tablet.

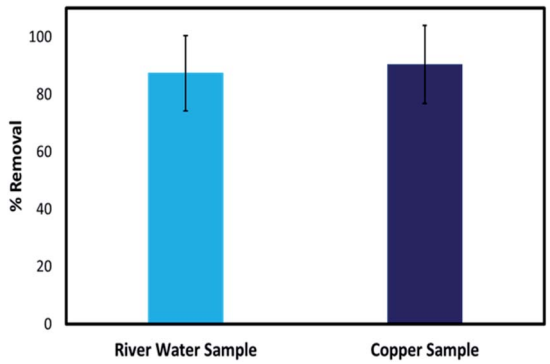

Fig. 11 Removal of Cu^{2+} from untreated river water sample that was spiked to create a 100 ppm Cu^{2+} solution, compared to the removal from a standard solution prepared in distilled water containing 100 ppm Cu^{2+}. Experiments were performed with one tablet after 18 h incubation.

tables were exposed to mixtures of the four highly adsorbing ions and compared to those exposed to each ion individually (Fig. 10). The data indicate the 3D printed tablets' capability to remove heavy metals, with similar removal capacities as for those with individual ions even when other ions are present. They also indicate that the co-existing metal ions are not competing for the same binding sites nor displace the highly adsorbing Cu^{2+} from the PEI binding sites. Therefore, the 3D printed tablets have the potential as a universal tool for the capture and removal of a variety of metal ions.

The printed tablets are stored in a dry state at room temperature until use with no sign of degradation over several months, and no special conditions are required for storage. It was found that the adsorption capacity remained unchanged after 240 days under the same testing conditions as described, which demonstrates excellent stability.

3.5 Application to an environmental water sample

The stability of the 3D printed tablets in actual environmental water was first investigated by incubating the tablets in raw water collected from the Raquette River, Potsdam, NY. When incubated in the water, the hydrogel tablets were robust and did not show any changes over time. The tablets were further tested from the removal of Cu^{2+} in spiked river water. Since the river water had no detectable levels of Cu^{2+} for the removal test, it was spiked with 100 ppm Cu^{2+}. As with distilled water, the color of the tablets changed to blue, and the tablets were able to remove 87.30% of the total Cu^{2+}, close to that obtained for a standard solution prepared in distilled water which showed 90.37% removal. This demonstrates that the removal performance of the tablets in a real water sample is comparable to the performance in laboratory samples and shows the feasibility of using these adsorbents in real environmental samples (Fig. 11).

4. Conclusion

The rapid advancement of additive manufacturing and 3D printing technologies has opened the door for the fabrication of complex functional products using fully automated manufacturing processes. We have developed a new printable adsorbent ink and 3D printing method for fabricating hydrogel-based tablets for use in heavy metal remediation. These 3D printed hydrogels are insoluble in water after the metal ion removal, which leads to easy recovery of the tablets. Several advantages are achieved using this approach. First, the printing method is scalable, and the materials used to formulate the ink are biodegradable and inexpensive. Second, the ink has the metal-binding ability through the PEI. These tablets utilize the strong crosslinking properties between PEI and metal ions to capture the ions from the environment. Third, the 3D printed hydrogel provides a simple method for removal using the 3D printed hydrogel tablets. The composition of the tri-polymer 3D printable ink includes sodium alginate, gelatin, and PEI, which together provide an excellent composite material system for capturing heavy metal ions, easily accessible and environmentally sustainable. Forth, we have shown that in addition to Cu^{2+} removal, they could be used for removing other heavy metal ions like cadmium, nickel, lead, and cobalt. The tablets and the adsorbent inks can be used for environmental remediation to help treat polluted wastewater, particularly in areas with high heavy metal concentrations in agricultural or industrial settings.

The results indicate the effect of achieving multi-functionality and increasing stability through reinforcing the hydrogel with PEI and demonstrate that the hydrogel composition and its rheology are essential factors in determining the printability, stability, and functionality of the hydrogel. An improved understanding of the factors regulating the stability of these hydrogels will allow further development of 3D printable formulations and manufacturing processes for a variety of applications in the environment and other fields. These findings are likely to be important when utilizing these materials and methods as green adsorbents for heavy metals and potentially other contaminants removal. This novel and cost-effective approach could help fabricate inexpensive systems for environmental decontamination.

Conflicts of interest

All authors have approved the final version of the manuscript. The authors declare no competing financial interest.

Acknowledgements

This work was funded by the National Science Foundation under Grants No. 1561491 and 2141017. Any opinions, findings, and conclusions or recommendations expressed in this material are those of the author(s) and do not necessarily reflect the views of the National Science Foundation. The authors thank Dr Daniel Andreescu (Chemistry and Biomolecular Science, Clarkson University) for the help with the AAS. The authors thank Dr Xiaocun Lu (Chemistry and Biomolecular Science, Clarkson University) for providing access to the rheometer (Anton Paar Modular Compact Rheometer MCR 302) and for their help with the rheology tests. The authors also thank Dr

Philip Yuya (Department of Mechanical and Aeronautical Engineering, Clarkson University) and Janith Wanniarachchi (Department of Mechanical and Aeronautical Engineering, Clarkson University) for providing access to the nano-mechanical testing instrument (TI-950 Triboindenter, Hysitron Inc.) and for their help with the nanoindentation tests. The authors also thank Dr Devon Shipp (Chemistry and Biomolecular Science, Clarkson University) and the Shipp Research Group for providing access to the tensile testing equipment. The authors also thank Mohamed Hassan and Shefa Alomari for helping with the BET analysis.

References

1 P. H. Gleick, Global freshwater resources: Soft-path solutions for the 21st century, *Science*, 2003, **302**, 1524–1528.
2 WHO, **https://www.who.int/en/news-room/fact-sheets/detail/drinking-water**.
3 J. Briffa, E. Sinagra and R. Blundell, Heavy metal pollution in the environment and their toxicological effects on humans, *Heliyon*, 2020, **6**, e04691.
4 N. S. Chary, C. T. Kamala and D. S. S. Raj, Assessing risk of heavy metals from consuming food grown on sewage irrigated soils and food chain transfer, *Ecotoxicol. Environ. Saf.*, 2008, **69**, 513–524.
5 P. B. Tchounwou, C. G. Yedjou, A. K. Patlolla and D. J. Sutton, Heavy metal toxicity and the environment, *Experientia Suppl.*, 2012, **101**, 133–164.
6 P. K. Rai, S. S. Lee, M. Zhang, Y. F. Tsang and K. H. Kim, Heavy metals in food crops: health risks, fate, mechanisms, and management, *Environ. Int.*, 2019, **125**, 365–385.
7 M. N. Khan, A. A. Wasim, A. Sarwar and M. F. Rasheed, Assessment of heavy metal toxicants in the roadside soil along the N-5, National Highway, Pakistan, *Environ. Monit. Assess.*, 2011, **182**, 587–595.
8 M. Rehman, L. J. Liu, Q. Wang, M. H. Saleem, S. Bashir, S. Ullah and D. X. Peng, Copper environmental toxicology, recent advances, and future outlook: a review, *Environ. Sci. Pollut. Res.*, 2019, **26**, 18003–18016.
9 V. Masindi and K. L. Muedi, Environmental contamination by heavy metals, *Heavy Metals*, 2018, **10**, 115–132.
10 M. Soleimani, N. Amini, B. Sadeghian, D. Wang and L. Fang, Heavy metals and their source identification in particulate matter (PM2.5) in Isfahan City, Iran, *J. Environ. Sci.*, 2018, **72**, 166–175.
11 J. Briffa, E. Sinagra and R. Blundell, Heavy metal pollution in the environment and their toxicological effects on humans, *Heliyon*, 2020, **6**, e04691.
12 I. Yruela, Copper in plants: acquisition, transport and interactions, *Funct. Plant Biol.*, 2009, **36**, 409–430.
13 L. M. FloresVelez, J. Ducaroir, A. M. Jaunet and M. Robert, Study of the distribution of copper in an acid sandy vineyard soil by three different methods, *Eur. J. Soil Sci.*, 1996, **47**, 523–532.
14 J. K. Xu, L. X. Yang, Z. Q. Wang, G. C. Dong, H. Y. Huang and Y. L. Wang, Toxicity of copper on rice growth and accumulation of copper in rice grain in copper contaminated soil, *Chemosphere*, 2006, **62**, 602–607.
15 F. L. Fu and Q. Wang, Removal of heavy metal ions from wastewaters: A review, *J. Environ. Manage.*, 2011, **92**, 407–418.
16 N. A. A. Qasem, R. H. Mohammed and D. U. Lawal, Removal of heavy metal ions from wastewater: a comprehensive and critical review, *npj Clean Water*, 2021, **4**, 1–15.
17 H. N. Tran, S. J. You, A. Hosseini-Bandegharaei and H. P. Chao, Mistakes and inconsistencies regarding adsorption of contaminants from aqueous solutions: A critical review, *Water Res.*, 2017, **120**, 88–116.
18 M. Barakat and N. Sahiner, Cationic hydrogels for toxic arsenate removal from aqueous environment, *J. Environ. Manage.*, 2008, **88**, 955–961.
19 O. Ozay, S. Ekici, Y. Baran, N. Aktas and N. Sahiner, Removal of toxic metal ions with magnetic hydrogels, *Water Res.*, 2009, **43**, 4403–4411.
20 A. S. Finny, O. Popoola and S. Andreescu, 3D-Printable Nanocellulose-Based Functional Materials: Fundamentals and Applications, *Nanomaterials*, 2021, **11**, 2358.
21 D. Zhao, Y. Liu, B. Liu, Z. Chen, G. Nian, S. Qu and W. Yang, 3D Printing Method for Tough Multifunctional Particle-Based Double-Network Hydrogels, *ACS Appl. Mater. Interfaces*, 2021, **13**, 13714–13723.
22 Z. Chen, D. H. Zhao, B. H. Liu, G. D. Nian, X. K. Li, J. Yin, S. X. Qu and W. Yang, 3D Printing of Multifunctional Hydrogels, *Adv. Funct. Mater.*, 2019, **29**, 1900971.
23 A. Masud, C. Zhou and N. Aich, Emerging investigator series: 3D printed graphene-biopolymer aerogels for water contaminant removal: a proof of concept, *Environ. Sci.: Nano*, 2021, **8**, 399–414.
24 A. S. Finny, C. Jiang and S. Andreescu, 3D Printed Hydrogel-Based Sensors for Quantifying UV Exposure, *ACS Appl. Mater. Interfaces*, 2020, **12**, 43911–43920.
25 W. Aljohani, M. W. Ullah, X. L. Zhang and G. Yang, Bioprinting and its applications in tissue engineering and regenerative medicine, *Int. J. Biol. Macromol.*, 2018, **107**, 261–275.
26 J. L. Wang, Y. Liu, X. T. Zhang, S. E. Rahman, S. H. Su, J. H. Wei, F. D. Ning, Z. L. Hu, R. Martinez-Zaguilan, S. R. Sennoune, W. L. Cong, G. Christopher, K. Zhang and J. J. Qiu, 3D printed agar/calcium alginate hydrogels with high shape fidelity and tailorable mechanical properties, *Polymer*, 2021, **214**, 1–9.
27 X. P. Gao, C. Guo, J. J. Hao, Z. Zhao, H. M. Long and M. Y. Li, Adsorption of heavy metal ions by sodium alginate based adsorbent-a review and new perspectives, *Int. J. Biol. Macromol.*, 2020, **164**, 4423–4434.
28 K. A. Kirk and S. Andreescu, Easy-to-Use Sensors for Field Monitoring of Copper Contamination in Water and Pesticide-Sprayed Plants, *Anal. Chem.*, 2019, **91**, 13892–13899.
29 D. H. Zhao, Y. D. Liu, B. H. Liu, Z. Chen, G. D. Nian, S. X. Qu and W. Yang, 3D Printing Method for Tough Multifunctional Particle-Based Double-Network Hydrogels, *ACS Appl. Mater. Interfaces*, 2021, **13**, 13714–13723.

30 J. Shojaeiarani, A. Shirzadifar and D. S. Bajwa, Robust and porous 3D-printed multifunctional hydrogels for efficient removal of cationic and anionic dyes from aqueous solution, *Microporous Mesoporous Mater.*, 2021, **327**, 111382.
31 M. Di Giuseppe, N. Law, B. Webb, R. A. Macrae, L. J. Liew, T. B. Sercombe, R. J. Dilley and B. J. Doyle, Mechanical behaviour of alginate-gelatin hydrogels for 3D bioprinting, *J. Mech. Behav. Biomed.*, 2018, **79**, 150–157.
32 M. Rajabi, M. McConnell, J. Cabral and M. A. Ali, Chitosan hydrogels in 3D printing for biomedical applications, *Carbohydr. Polym.*, 2021, **260**, 117768.
33 S. R. Derkach, N. G. Voron'ko, N. I. Sokolan, D. S. Kolotova and Y. A. Kuchina, Interactions between gelatin and sodium alginate: UV and FTIR studies, *J. Dispers. Sci. Technol.*, 2020, **41**, 690–698.
34 F. Bucatariu, C. A. Ghiorghita, M. M. Zaharia, S. Schwarz, F. Simon and M. Mihai, Removal and Separation of Heavy Metal Ions from Multicomponent Simulated Waters Using Silica/Polyethyleneimine Composite Microparticles, *ACS Appl. Mater. Interfaces*, 2020, **12**, 37585–37596.
35 H. J. Kong and D. J. Mooney, The effects of poly(ethyleneimine) (PEI) molecular weight on reinforcement of alginate hydrogels, *Cell Transplant.*, 2003, **12**, 779–785.
36 W. Luo, Z. Bai and Y. Zhu, Fast removal of Co(ii) from aqueous solution using porous carboxymethyl chitosan beads and its adsorption mechanism, *RSC Adv.*, 2018, **8**, 13370–13387.
37 Y.-Z. Yan, Q.-D. An, Z.-Y. Xiao, S.-R. Zhai, B. Zhai and Z. Shi, Interior multi-cavity/surface engineering of alginate hydrogels with polyethylenimine for highly efficient chromium removal in batch and continuous aqueous systems, *J. Mater. Chem. A*, 2017, **5**, 17073–17087.
38 H. Y. Zhu, Y. Q. Fu, R. Jiang, J. Yao, L. Xiao and G. M. Zeng, Optimization of Copper(II) Adsorption onto Novel Magnetic Calcium Alginate/Maghemite Hydrogel Beads Using Response Surface Methodology, *Ind. Eng. Chem. Res.*, 2014, **53**, 4059–4066.
39 N. Li and R. B. Bai, Copper adsorption on chitosan-cellulose hydrogel beads: behaviors and mechanisms, *Sep. Purif. Technol.*, 2005, **42**, 237–247.
40 Y. J. Dong, D. S. Sang, C. D. He, X. F. Sheng and L. W. Lei, Mxene/alginate composites for lead and copper ion removal from aqueous solutions, *RSC Adv.*, 2019, **9**, 29015–29022.
41 P. C. Bandara, E. T. Nadres and D. F. Rodrigues, Use of Response Surface Methodology To Develop and Optimize the Composition of a Chitosan-Polyethyleneimine-Graphene Oxide Nanocomposite Membrane Coating To More Effectively Remove Cr(VI) and Cu(II) from Water, *ACS Appl. Mater. Interfaces*, 2019, **11**, 17784–17795.
42 M. Pishnamazi, S. Ghasemi, A. Khosravi, A. ZabihiSahebi, A. Hasan-Zadeh and S. M. Borghei, Removal of Cu (ll) from industrial wastewater using poly (acrylamide-co-2-acrylamide-2-methyl propane sulfonic acid)/graphene oxide/sodium alginate hydrogel: Isotherm, kinetics, and optimization study, *J. Water Proc. Eng.*, 2021, 42.
43 F. Wang, T. Duo, Y. Wang, Z. Xiao, A. Xu and R. Liu, Novel Polyethyleneimine/κ-Carrageenan Composite from Facile One-Step Fabrication for the Removal of Copper Ion from Aqueous Solution, *J. Polym. Environ.*, 2021, **30**, 1001–1011.